

Evolution and stability of spatial solitons in a photorefractive two-wave mixing system*

Liu Jin-Song(刘劲松)[†], Zhang Hui-Lan(张慧蓝),
Zhang Guang-Yong(张光勇), and Wang Cheng(王程)

State Key Laboratory of Laser Technology, Huazhong University of Science and Technology, Wuhan 430074, China

(Received 1 August 2005; revised manuscript received 7 November 2005)

The dynamical evolution and stability of bright dissipative holographic solitons in biased photorefractive materials in which the self-trapping beam obtains a gain from the pump beam via two-wave mixing has been investigated numerically. Results show that these solitons are stable relative to small perturbations. Adjusting some system parameters, such as the bias field and the angle between beams, can easily control the generation of such solitons. Potential applications in optical switches or repeaters are discussed.

Keywords: spatial optical solitons, photorefractive nonlinear optics, two-wave mixing

PACC: 4265J, 4265S

1. Introduction

Optical spatial solitons have been studied extensively.^[1–22] One way to generate spatial optical solitons is to use an interference pattern with and without energy exchange for both bright and dark cases,^[1–6] which can be divided into two categories: first, the interference of two beams is used to generate a periodic spatial pattern and then the pattern is injected into a medium to form a periodic array of dark solitons.^[1–3] For example, the generation of a periodic array of dark spatial solitons from two plane waves propagating at some angle in the regime of adiabatic amplification was demonstrated in a Kerr-like medium^[1,2] in which the combined action of nonlinearity, diffraction, and amplification lead to the reshaping of the input signal into an array of dark solitons with flat phase fronts in the bright background region. Such arrays of dark spatial solitons were also demonstrated in photorefractive (PR) crystal $\text{Bi}_{12}\text{TiO}_{20}$.^[3] Second, the interference of two beams is used to create a focusing effect via two-wave mixing in a medium.^[4] It has been proven theoretically that such an effect, called the holographic focusing effect, could make one or two of the beams evolve into spatial soliton with or without energy exchange be-

tween beams for both bright and dark cases.^[5,6] Holographic focusing effect was already observed in PR media, in which a mutual focusing/defocusing of two beams with slightly different frequencies was demonstrated with a biased SBN (strontium barium niobate) crystal.^[4]

The mechanism to form the holographic focusing effect arises from a grating in the refractive index induced by interference between two beams (i.e., the signal and pump beams) via two-wave mixing. Through the grating (i.e., the induced periodic modulation of the refractive index) the beams are coupled through Bragg reflections. Each beam is Bragg reflected and coherently added into the other beam. This can lead to focusing of narrow beams when the reflected beams are $\pi/2$ phase retarded with respect to the primary beams. It was proposed that the two beams could evolve into spatial solitons simultaneously based on the holographic focusing mechanism for both bright and dark cases, and consequently such solitons were called holographic solitons.^[5] Because a holographic soliton consists of two mutually coherent field components, holographic solitons are existent as a pair. The presence of both components is required, since each beam alone cannot survive as a soliton if the other beam is absent. The condition to form holographic

*Project supported by the National Natural Science Foundation of China (Grant No 10574051).

[†]Corresponding Author: E-mail: jslu4508@vip.sina.com

solitons is that the asymmetric energy exchange between the beams does not take place. Such a condition is necessary when the two beams are going to evolve into spatial solitons simultaneously. The asymmetric energy exchange from the pump beam to the signal beam allows the signal beam to obtain a gain and the pump beam to obtain a negative gain. Although it is possible for the gain to be balanced by the loss of the signal beam, thus making it possible for the signal beam to evolve into a soliton, it is not possible for the negative gain to be balanced by any factor for the pump beam. This means that the pump beam cannot evolve into a soliton. Therefore the two beams can evolve into holographic solitons simultaneously only if the asymmetric energy exchange does not take place. It was proposed that,^[6] when the asymmetric energy exchange took place, the signal beam alone could evolve into a new kind of holographic solitons in both bright and dark cases in such a configuration where the pump beam was of a uniform spatial distribution in both transverse dimensions and much stronger than the signal beam, whereas the signal beam, i.e. the self-trapping beam, had a one-dimensional (1D) soliton-like spatial distribution and could obtain a gain from the pump beam via wave mixing between the beams. Because this configuration could amplify or absorb the signal beam, it was a dissipative system. Inasmuch as this, the new kind of holographic solitons was called dissipative holographic (DH) solitons.^[6]

DH solitons are produced in dissipative systems in which soliton solutions result from a double balance, i.e. diffraction is balanced by nonlinearity and loss is balanced by gain. The double balance results in soliton solutions with fixed amplitude and width for fixed values of system parameters.^[6,7] Meanwhile, DH solitons can effectively overcome the effect of absorption. These features may provide efficient suppression of noise and stop any drift in the soliton parameters and will be useful for application in soliton-driven photonics, such as an optical switch or repeater. In order to find applications of DH solitons, it is necessary to investigate the dynamical evolution and stability of bright DH solitons as well as to determine which system parameter can be used to control the generation of solitons. For this purpose, this paper provides a comprehensive numerical study on these issues by using beam propagation methods in steady state under the undepleted pump condition. Our results show that bright DH solitons are stable against small per-

turbations and have a number of possible applications ranging from optical switch to repeater.

2. Theoretical model

Consider the schematic shown in Fig.1. The PR crystal proposed here is SBN with its optical c -axis oriented along the y -axis. The signal and pump beams are arranged to propagate in the crystal and each beam makes a small angle (θ) of its k vector with the z -axis. The signal beam has a 1D bright soliton-like spatial distribution that is confined in the x direction, whereas it is extended (nondiffracting) in the y direction. The pump beam has a uniform spatial distribution in both x and y directions. Both signal and pump beams are extraordinary-polarized. The two coherent beams couple each other by PR two-wave mixing with a biased field applied along the y direction, i.e. normal to the narrow direction of the signal beam. As a result, in this configuration, there are no focusing effects in x direction induced by the photorefractive screening nonlinearity.

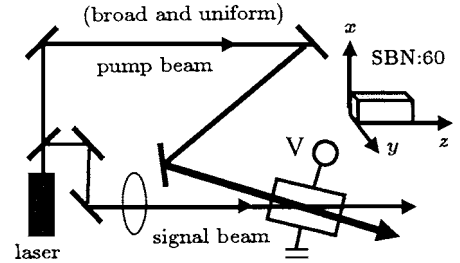


Fig.1. Schematic of a dissipative holographic soliton produced in a biased PR crystal. Signal and pump beams couple each other by PR two-wave mixing.

Let ϕ denote the slowly varying envelopes of the electric-field component of the signal beam. In the slowly-varying approximation, ϕ satisfies the following paraxial wave equation:^[6]

$$\frac{1}{2k} \frac{\partial^2 \phi}{\partial x^2} + i \cos \theta \frac{\partial \phi}{\partial z} + \left(\Gamma_0 - \frac{i}{2} \Gamma \right) \frac{I_p}{I_p + I} \phi + i \frac{1}{2} \alpha_0 \phi = 0, \quad (1)$$

where $k = n_e k_0$, $k_0 = 2\pi/\lambda_0$ and λ_0 is the free-space wavelength of the light wave employed, n_e is the extraordinary refractive index, α_0 is the absorption coefficient of the crystal, Γ and Γ_0 are the intensity and phase coupling coefficients of the two-wave mixing, respectively, I_p is the intensity of the pump beam, $I(x, z) = (n_e/2\eta_0) |\phi(x, z)|^2$, and $\eta_0 = (\mu_0/\epsilon_0)^{1/2}$. Let $U = (2\eta_0 I_p/n_e)^{-1/2} \phi$, under the condition $|U|^2 = I/I_p \ll 1$. From Eq.(1) we can obtain a dynamical

evolution equation in term of U as follows:

$$i \frac{\partial U}{\partial \xi} + \frac{1}{2} \frac{\partial^2 U}{\partial s^2} + (g_0 - iG)U - (g_0 - ig)U |U|^2 = 0, \quad (2)$$

where $s = x/x_0$, $\xi = z/(z_0 \cos \theta)$, $z_0 = kx_0^2$, x_0 is an arbitrary spatial width, $g_0 = z_0 \Gamma_0$, $g = z_0 \Gamma/2$, $\alpha = z_0 \alpha_0/2$, and $G = g - \alpha$ denotes a net gain. By use of the results reported in Ref.[7], the bright and dark soliton solutions of Eq.(2) were obtained in Ref.[6], and the expression of bright one is rewritten as

$$U(s, \xi) = F \operatorname{sech}(Bs) \exp\{i b \ln[\operatorname{sech}(Bs)]\} \exp(-i\nu \xi), \quad (3)$$

where $F = [3G/(2g)]^{1/2}$ is the amplitude, $B = (G/b)^{1/2}$ is the parameter associated with the width, $b = [3g_0 + (9g_0^2 + 8g^2)^{1/2}]/(2g)$ is the chirp parameter, $\nu = (b^2 - 1)G/(2b) - g_0$ denotes the nonlinear shifts of the propagation constant. For the PR two-wave mixing process with a biased field, g and g_0 can be expressed as^[23]

$$g = \delta \frac{E_0^2 + E_d(E_d + E_s)}{(E_d + E_s)^2 + E_0^2} E_s, \quad (4)$$

$$g_0 = \delta \frac{E_0 E_s}{(E_d + E_s)^2 + E_0^2} E_s, \quad (5)$$

where E_0 is the bias field, $E_d = 4\pi k_B T \sin \theta / (\lambda_0 e)$ is the diffusion field, $E_s = e N_A \lambda_0 / (4\pi \epsilon_r \epsilon_0 \sin \theta)$ is the saturation field, N_A is the acceptor density, ϵ_r and ϵ_0 are the effective dielectric constant and the permittivity of vacuum, respectively, k_B is the Boltzmann constant, e is the electron charge, T is the absolute temperature, $\delta = (n_e^2 k_0 x_0)^2 \gamma_{\text{eff}}/2$, and γ_{eff} is the effective electro-optic coefficient. For the configuration shown in Fig.1, we have $\gamma_{\text{eff}} = \bar{n}^3 \gamma_{33} \cos^2 \theta -$

$\bar{n}^{-1} \gamma_{13} \sin^2 \theta$, where $\bar{n} = n_e/n_0$, n_0 is the ordinary refractive index.^[24]

3. Evolution and stability

3.1. Propagation of bright DH soliton

In order to give some actual examples, the parameters of a SNB:60 crystal at $\lambda_0 = 0.5 \mu\text{m}$ and $T = 300\text{K}$ are taken as $n_e = 2.35$, $n_o = 2.37$, $\gamma_{13} = 47 \text{pm/V}$, $\gamma_{33} = 235 \text{pm/V}$, and $\epsilon = 880$.^[25] Taking $E_0 = -1700 \text{V/cm}$, $2\theta = 0.1^\circ$, $N_A = 5 \times 10^{17} \text{cm}^{-3}$, $\alpha_0 = 0.45 \text{cm}^{-1}$ and $x_0 = 25 \mu\text{m}$, those dimensionless system parameters in Eq.(2) are $\alpha = 0.415$, $g = 0.434$ and $g_0 = -58.6$, which makes $G = 1.86 \times 10^{-2}$. Furthermore, these values make $z_0 \approx 1.85$, thus meaning $\xi = 1$ corresponding to $z \approx 1.85 \text{cm}$ for a very small value of θ . The corresponding values of Γ and Γ_0 in Eq.(1) are $\Gamma = 0.47 \text{cm}^{-1}$ and $\Gamma_0 = -32 \text{cm}^{-1}$. For these values, from Eq.(3), we have a DH bright soliton with $F = F_0 = 0.245$, $B = B_0 = 1.94$, $b = b_0 = 4.93 \times 10^{-3}$ and $\nu = \nu_0 = 56.7$. The intensity FWHM of this soliton is $22 \mu\text{m}$ and the peak value of I_s/I_p is 0.06. The dynamical evolution of such a bright DH soliton can be obtained by numerically solving Eq.(2). As expected, our results confirm that the bright soliton state remains invariant with propagation distance (calculated for $\xi = 5$, i.e. $z \approx 9.2 \text{cm}$), as shown in Fig.2(a). The other two examples with different combinations of system parameters are also shown in Fig.2(b) with $E_0 = -50 \text{V/cm}$ and $\alpha_0 = 0.417 \text{cm}^{-1}$, and in Fig.2(c) with $E_0 = -2200 \text{V/cm}$ and $\alpha_0 = 0.488 \text{cm}^{-1}$. Note that the values of θ , N_A , and x_0 for the last two examples are taken as the same as that for the first example.

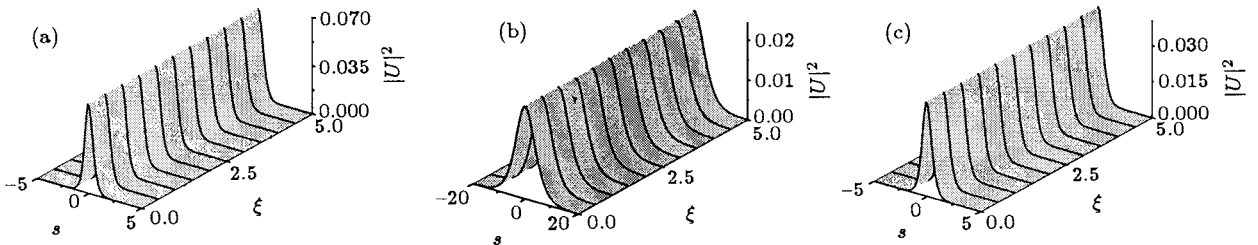


Fig.2. Simultaneous propagation of DH bright solitons (intensity profiles). (a) System parameters: $\alpha = 0.415$, $g = 0.434$, and $g_0 = -58.6$. Soliton parameters: $F = 0.245$, $B = 1.94$, $b = 4.93 \times 10^{-3}$ and $\nu = 56.7$. (b) System parameters: $\alpha = 0.385$, $g = 0.391$, and $g_0 = -1.72$. Soliton parameters: $F = 0.152$, $B = 0.201$, $b = 0.150$ and $\nu = 1.70$. (c) System parameters: $\alpha = 0.450$, $g = 0.462$, and $g_0 = -75.9$. Soliton parameters: $F = 0.199$, $B = 1.73$, $b = 4.06 \times 10^{-3}$ and $\nu = 74.4$.

3.2. Stability of bright DH solitons

In this section we investigate the stability of DH solitons relative to small perturbations in the initial

conditions. We pay our attention on the DH bright soliton shown in Fig.2(a) with soliton parameters $F = F_0 = 0.245$, $B = B_0 = 1.94$, $b = b_0 = 4.93 \times 10^{-3}$ and $\nu = \nu_0 = 56.7$. In order to introduce the perturba-

tions in the initial conditions, taking $F = F_0 + \Delta F$, $B = B_0 + \Delta B$, $b = b_0$, and $\nu = \nu_0$ in Eq.(3), we can obtain a beam whose amplitude and width are slightly different from those of the exact DH bright soliton solution shown in Fig.2(a). The evolution of this beam can be obtained by solving Eq.(2) with the system parameters $\alpha = 0.415$, $g = 0.434$, and $g_0 = -58.6$. Figure 3 gives two examples for $\Delta F/F_0 = 1\%$ and $\Delta B = 0$ as well as $\Delta F = 0$ and $\Delta B/B_0 = -1\%$, respectively, in which the beams reshape themselves

and try to evolve into a solitary wave. We make a more comprehensive calculation to investigate the evolutions of the peak intensity and the intensity FWHM for different values of $|\Delta F/F_0|$ and $|\Delta B/B_0|$ with the system parameters above, as shown in Fig.4. Results indicate that this soliton is stable when $|\Delta F/F_0| \leq 1\%$ and $\Delta B = 0$ as well as $\Delta F = 0$ and $|\Delta B/B_0| \leq 1\%$. These results indicate that DH solitons are stable against small perturbations.

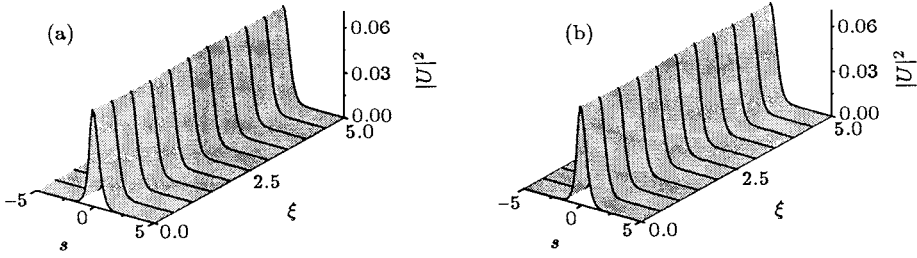


Fig.3. Dynamical evolution towards the solitary wave (intensity profiles). System and soliton parameters are the same as those in Fig.2(a). Input conditions: (a) $\Delta F/F_0 = -1\%$ and $\Delta B = 0$. (b) $\Delta F = 0$ and $\Delta B/B_0 = 1\%$.

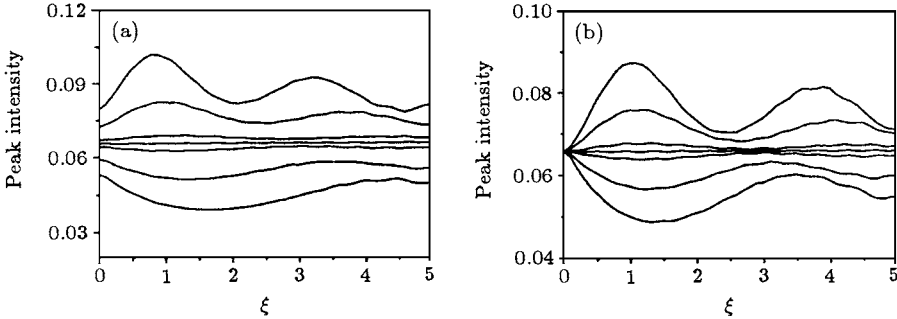


Fig.4. Dynamical evolution of peak intensity. System and soliton parameters are the same as those in Fig.2(a). Input conditions: (a) $\Delta B = 0$ and $\Delta F/F_0 = 10\%$, 5% , 1% , 0 , -1% , -5% , and -10% (from top to bottom). (b) $\Delta F = 0$ and $\Delta B/B_0 = -10\%$, -5% , -1% , 0 , 1% , 5% , and 10% (from top to bottom).

4. Effects of system parameters on the propagation of DH bright solitons

For the SBN: 60 crystal given above, when $E_0 = -1700\text{V/cm}$, $2\theta = 0.1^\circ$, $N_A = 5 \times 10^{17}\text{cm}^{-3}$, $\alpha_0 = 0.45\text{cm}^{-1}$ and $x_0 = 25\mu\text{m}$, we have obtained a set of system parameter as $\alpha = 0.415$, $g = 0.434$ and $g_0 = -58.6$ with a net gain $G = G_0 = 1.86 \times 10^{-2}$, which support a DH bright soliton with $F = F_0 = 0.245$, $B = B_0 = 1.94$, $b = b_0 = 4.93 \times 10^{-3}$ and $\nu = \nu_0 = 56.7$ as shown in Fig.2(a). Letting this solitary wave be the input beam, in this section, by numerically solving Eq.(2), we investigate the dynamical evolution of the beam in the SBN: 60 crystal at different values of α , E_0 or θ that will give different

values of system parameters α , g and g_0 , from which we can obtain the information about how to control the generation of this incident solitary beam by adjusting α , E_0 or θ .

4.1. Effects of absorption

Firstly, we consider the influence of the linear loss α on the propagation of the incident solitary beam in the SBN for $E_0 = -1700\text{V/cm}$ and $2\theta = 0.1^\circ$. The net gain $G = g - \alpha$ varies with α . As mention above, $G = G_0 = 1.86 \times 10^{-2}$ when $\alpha = 0.415$. Let $\Delta G = G - G_0$ denote the variation in the net gain when $\alpha \neq 0.415$. The dynamical evolution of the incident beam in the crystal is depicted in Fig.5 for $g = 0.434$, $g_0 = -58.6$ and $\alpha = 0.35$, 0.41 , 0.5 and 0.6 , which make $\Delta G = 0.0654$, 0.00538 , -0.0846 ,

and -0.185 , respectively. These results show that the beam exhibits different behaviours of evolution for different sign of ΔG . When $\Delta G < 0$, which corresponds to the excess loss case, the intensity of the beam decreases with propagation distance because the gain cannot overcome the loss and then the beam is progressively absorbed as it propagates and, consequently, the beam cannot evolve into a bright DH soliton irrespective of how large $|\Delta G|$ is, as shown in Figs.5(a) and 5(b). However, when $\Delta G > 0$, which corresponds to the excess gain case, the beam peak intensity increases and the beam width decreases

with propagation distance, and both the intensity and width vary with propagation distance in a fashion of periodic oscillation, and then the beam cannot evolve into a stable DH bright soliton for a big value of ΔG , such as $\Delta G = 0.0654$, as shown in Fig.5(c). The beam tends to experience one cycle of expansion and compression, and its peak intensity decreases initially and then increases with propagation distance, and both the intensity and width of the beam finally reach a saturation value, and the beam finally evolves into a stable DH soliton for a small value of ΔG , such as $\Delta G = 0.00538$, as shown in Fig.5(d).

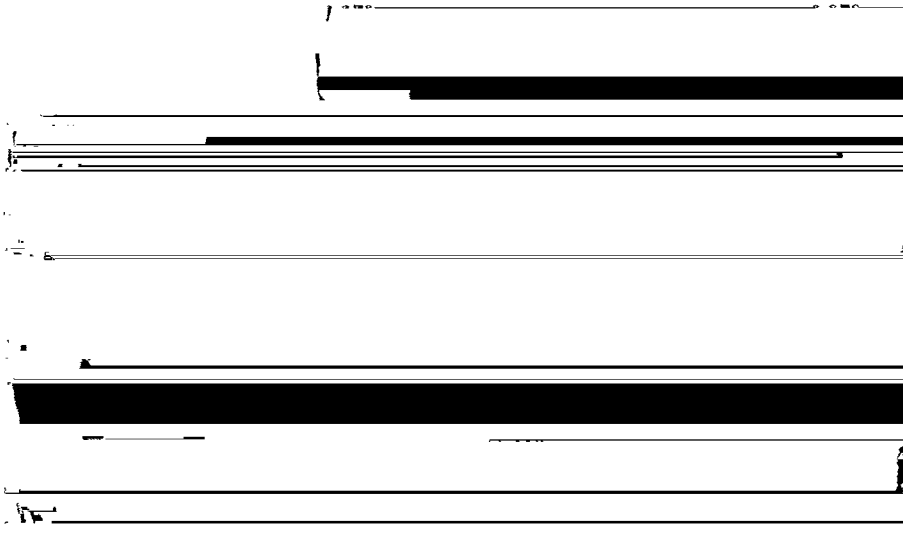


Fig.5. Effect of loss on the evolution of an incident solitary beam in a dissipative PR system. The incident beam is a bright DH solitary wave with $F = 0.245$, $B = 1.94$, $b = 4.93 \times 10^{-3}$ and $\nu = 56.7$. The system parameters are $g = 0.434$ and $g_0 = -58.6$ and (a) $\alpha = 0.5$, $\Delta G = -0.0846$; (b) $\alpha = 0.6$, $\Delta G = -0.185$; (c) $\alpha = 0.35$, $\Delta G = 0.0654$ and (d) $\alpha = 0.41$, $\Delta G = 0.00538$.

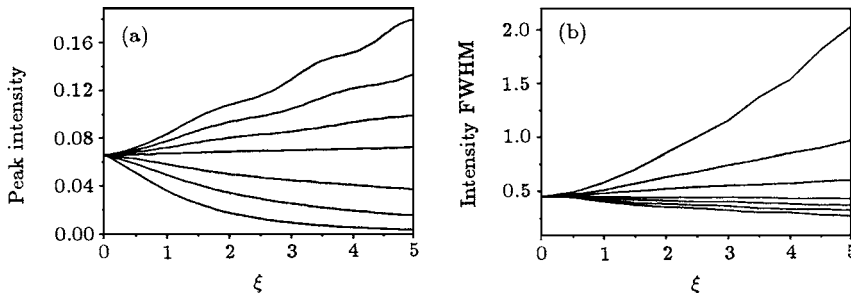


Fig.6. Effect of loss on the evolution of the peak intensity and intensity FWHM of an incident solitary beam in a dissipative PR system. The incident beam is a bright DH solitary wave with $F = 0.245$, $B = 1.94$, $b = 4.93 \times 10^{-3}$ and $\nu = 56.7$. The system parameters are $g = 0.434$ and $g_0 = -58.6$ (a) $\alpha = 0.35, 0.37, 0.39, 0.41, 0.45, 0.5, 0.6$ (from top to bottom) and (b) $\alpha = 0.6, 0.5, 0.45, 0.41, 0.39, 0.37, 0.35$ (from top to bottom).

In order to give a full view, Fig.6 depicts the evolution of the peak intensity and intensity FWHM. For the case of excess loss, the gain cannot overcome the loss and the focusing effect cannot balance the diffrac-

tion. The two imbalances make the intensity weaker and the width broader as the beam propagates, thus the beam cannot evolve into a soliton. For the case of excess gain, however, the gain exceeds the loss and

the focusing effect exceeds the diffraction, the two imbalances make the intensity stronger and the width narrower, thus the beam cannot evolve into a soliton, too, except for the case that the gain is near the loss, in which the beam can lose its energy until new balances are constructed and the beam finally evolves into a soliton with a stable spatial profile different from that of the incident beam.

4.2. Effects of bias field

We now consider the influence of the bias field E_0 on the propagation of the solitary beam in the SBN crystal for $\alpha = 0.415$ and $2\theta = 0.1^\circ$. Firstly, we consider the case that the value of $|E_0|$ is smaller than 1700 V/cm, such as $E_0 = -1600$ V/cm as well as $E_0 = -1150$ V/cm, and the corresponding values of g and g_0 are 0.429 and -55.2 as well as 0.411 and -39.7 ,

respectively. For this case, the values of g are smaller than that for $E_0 = -1700$ V/cm, which means this is an excess loss case, thus resulting in the beam intensity decreasing and the beam width increasing with propagation distance, because the gain cannot overcome the loss, and then the beam cannot evolve into a stable solitary wave. When the value of $|E_0|$ is far smaller than 1700 V/cm, such as $E_0 = -1150$ V/cm, the beam amplitude is progressively reduced, and the beam width expands initially and then tends to compress and expand periodically as it propagates, as shown in Figs.7(a) and 8; whereas the beam tends to experience a large cycle of compression and expansion, and its maximum amplitude oscillates with propagation distance when the value of $|E_0|$ is slightly smaller than 1700 V/cm, such as $E_0 = -1600$ V/cm, as shown in Figs.7(b) and 8.

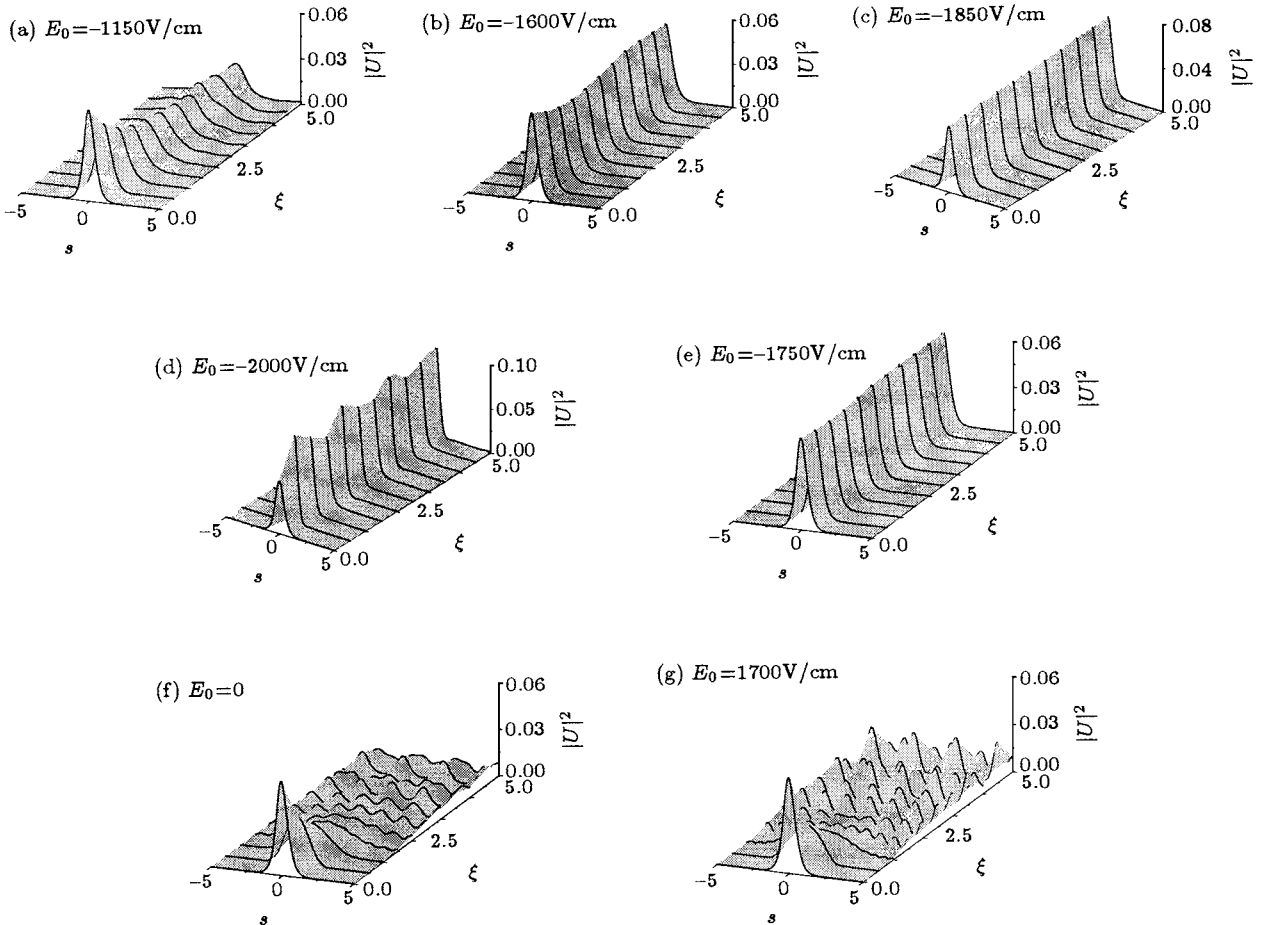


Fig.7. Effect of bias fields on the evolution of an incident solitary beam in a dissipative PR system. The incident beam is a bright DH solitary wave with $F = 0.245$, $B = 1.94$, $b = 4.93 \times 10^{-3}$ and $\nu = 56.7$. The system parameters are $\alpha = 0.415$ and (a) $g = 0.411$ and $g_0 = -39.7$; (b) $g = 0.429$ and $g_0 = -55.2$; (c) $g = 0.442$ and $g_0 = -63.8$; (d) $g = 0.450$ and $g_0 = -69.0$; (e) $g = 0.436$ and $g_0 = -60.3$; (f) $g = 0.391$ and $g_0 = 0$; (g) $g = 0.436$ and $g_0 = 58.6$.

We then consider the case that the value of $|E_0|$ is larger than 1700 V/cm, such as $E_0 = -2000$ V/cm as well as $E_0 = -1850$ V/cm, and the corresponding values of g and g_0 are 0.450 and -69.0 as well as 0.442 and -63.8 , respectively. For this case, the values of g are larger than that for $E_0 = -1700$ V/cm, which means this is an excess gain case; as a result, the beam intensity increases and the beam width decreases with propagation distance, and the beam is finally amplified. When the value of $|E_0|$ is slightly larger than 1700 V/cm, such as $E_0 = -1850$ V/cm, the intensity of the beam is incessantly amplified and the width of the beam is incessantly compressed as it propagates, as shown in Figs.7(c) and 8, whereas the beam tends to experience several cycles of compression and expansion, and its maximum amplitude oscillates with propagation distance when the value of $|E_0|$ is larger than 1700 V/cm enough, such as $E_0 = -2000$ V/cm, as shown in Figs.7(d) and 8.

If $|E_0|$ is larger than 1700 V/cm quite slightly, such as $E_0 = -1750$ V/cm, it gives $g = 0.436$ and $g_0 = -60.3$. Although this is still an excess gain case, the input beam initially experiences a cycle with its

width expanding and compressing and with its peak intensity decreasing and increasing, and finally both the width and intensity reach a stable value, finally the beam evolves into a stable soliton, as shown in Figs.7(e) and 8. If we turn the bias field off, i.e., let $E_0 = 0$, which gives $g = 0.391$ and $g_0 = 0$, and corresponds to an excess loss case, this beam will become a diverging wave as it propagates, as shown in Figs.7(f) and 8. When the incident beam is a DH bright soliton supported by the crystal parameters with $E_0 = -1700$ V/cm, if we turn the bias field from $E_0 = -1700$ V/cm to $E_0 = 1700$ V/cm, this beam still diverges as it propagates, as shown in Figs.7(g) and 8. For the last case, although the value of g keeps 0.434 unchanged, the value of g_0 changes from -58.6 to 58.6. Such system parameters can support a DH bright soliton with a quite broader width, and hence cannot support this input beam with quite narrower width to evolve into a soliton. In other words, for this case, the loss may be balanced by the gain, but the diffraction cannot be balanced by the focusing effect, thus resulting in the diverging of the beam.

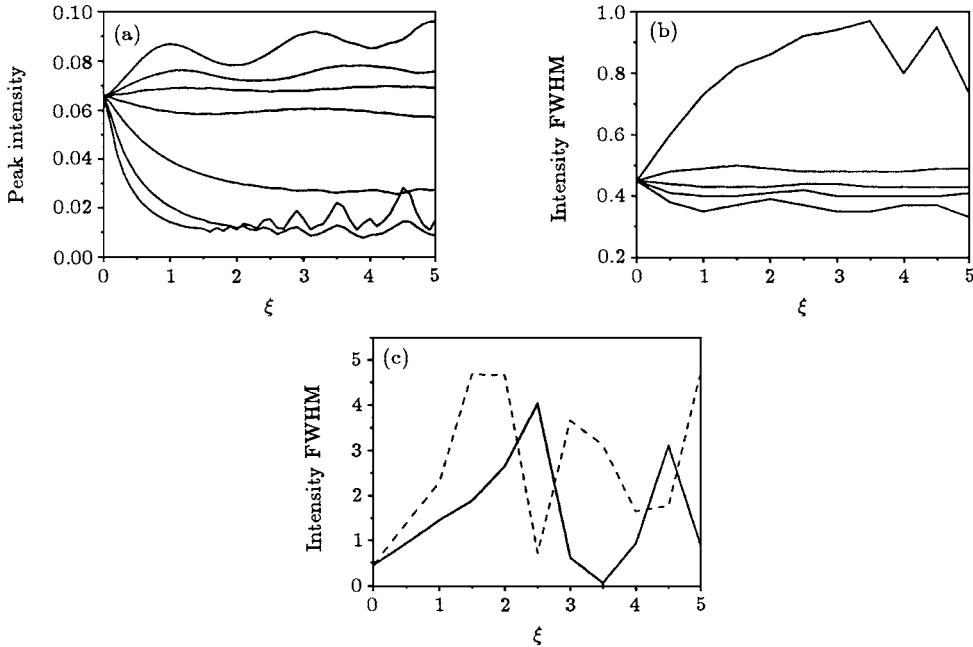


Fig.8. Effect of bias fields on the evolution of the peak intensity and intensity FWHM of an incident solitary beam in a dissipative PR system. The input beam is a bright DH solitary wave with $F = 0.245$, $B = 1.94$, $b = 4.93 \times 10^{-3}$ and $\nu = 56.7$. The system parameters are $\alpha = 0.415$, and (a) $E_0 = -2000, -1850, -1750, -1600, -1150, 1700, 0$ (from top to bottom), and (b) $E_0 = -1150, -1600, -1750, -1850, -2000$ (from top to bottom), (c) the dashed line for $E_0 = 1700$, and the solid line for $E_0 = 0$. The unit of E_0 is V/cm.

4.3. Effects of the angle between beams

Finally, we consider the influence of the angle be-

tween beams on the propagation of the incident solitary beam in the SBN crystal for $\alpha = 0.415$ and $E_0 = -1700$ V/cm as shown in Fig.9. We take five val-

ues of θ as 0.03° , 0.04° , 0.052° , 0.06° , and 0.07° . The corresponding values of g and g_0 are $g=0.260$, 0.347 , 0.451 , 0.521 , and 0.607 , respectively, and $g_0=-58.6$ for all the values of θ (in fact, the value of g_0 changes with θ very slightly). When $\theta > 0.05^\circ$, the system relative to the incident beam lies in an excess gain state, whereas lies in an excess loss state when $\theta < 0.05^\circ$. When θ is adjusted from 0.03° to 0.07° , the incident beam presents a behaviour of evolution in the crystal similar to that when the bias field is adjusted. That is,

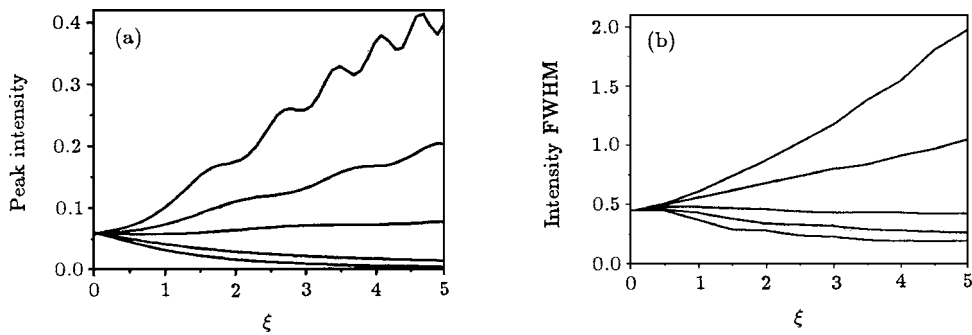


Fig.9. Effect of the angle between beams on the evolution of the peak intensity and intensity FWHM of an incident solitary beam in a dissipative PR system. The input beam is a bright DH solitary wave with $F = 0.245$, $B = 1.94$, $b = 4.93 \times 10^{-3}$ and $\nu = 56.7$. The system parameters are $\alpha = 0.415$, and (a) $\theta = 0.07^\circ$, 0.06° , 0.052° , 0.04° , and 0.03° (from top to bottom), and (b) $\theta = 0.03^\circ$, 0.04° , 0.052° , 0.06° , and 0.07° (from top to bottom).

5. Conclusion and discussion

The results obtained in Section 4 lead the dissipative PR systems that support DH bright solitons to a number of possible applications ranging from optical switches to optical repeaters. By adjusting the bias field, one can control the generation of a solitary beam in a dissipative PR system. If we regard the system as a state of turning on when $E_0 = -1700$ V/cm as shown in Fig.2(a), this system can be switched to the state of turning off when $E_0 = 0$ as shown in Fig.7(f). When $E_0 = -1150$ V/cm, the system is not completely closed, as shown in Fig.7(a). This prop-

erty may be promising in optical switching application. When $E_0 = -1850$ V/cm, the peak value of the solitary beam intensity is amplified from 0.06 at the input end to 0.07 at the output end, as shown in Fig.7(c). Such an amplification occurs when $E_0 < 0$ and $|E_0| > 1700$ V/cm, and the amplification ratio increases as $|E_0|$ increases. This property may be promising in optical repeating application.

In conclusion, dissipative holographic bright solitons supported by biased PR materials with two-wave mixing have been investigated. Perhaps some novel soliton-driven photonics could be made based on the results presented in this paper.

References

- [1] Bosshard C, Mamyshev P V and Stegeman G I 1994 *Opt. Lett.* **19** 90
- [2] Mamyshev P V, Bosshard C and Stegeman G I 1994 *J. Opt. Soc. Am. B* **11** 1254
- [3] Macuil R D and Castillo M D I 2003 *J. Opt. A: Pure Appl. Opt.* **5** S493
- [4] Vaupel M, Seror C and Dykstra R 1997 *Opt. Lett.* **22** 1470
- [5] Cohen O, Carmon T, Segev M and Odoulov S 2002 *Opt. Lett.* **27** 2031
- [6] Liu J S 2003 *Opt. Lett.* **28** 2237
- [7] Akhmediev N N, Afanasjev V V and Soto-Crespo J M 1996 *Phys. Rev. E* **53** 1190
- [8] Liu J S and Lu K Q 1998 *Acta Phys. Sin.* **47** 1509 (in Chinese)
- [9] Hou C F, Li S Q, Li B, Sun X D 2001 *Acta Phys. Sin.* **50** 73 (in Chinese)
- [10] Liu J S and Zhang D Y 2000 *Chin. Phys.* **9** 667
- [11] Liu J S 2001 *Chin. Phys.* **10** 1037

- [12] Liu J S and Zhang D Y 2001 *Acta Phys. Sin.* **50** 880 (in Chinese)
- [13] Hao Z H and Liu J S 2002 *Acta Phys. Sin.* **51** 818 (in Chinese)
- [14] Hao Z H and Liu J S 2002 *Acta Phys. Sin.* **51** 2772 (in Chinese)
- [15] Liu J S and Hao Z H 2002 *Chin. Phys.* **11** 254
- [16] He G G, Wang X S, She W L 2002 *Acta Phys. Sin.* **51** 2270 (in Chinese)
- [17] Liu J S and Hao Z H 2003 *Chin. Phys.* **12** 1124
- [18] Liu J S 2004 *Acta Phys. Sin.* **53** 3014 (in Chinese)
- [19] Liu J S and Hao Z H 2004 *Chin. Phys.* **13** 704
- [20] Wang X H and Gou Q 2005 *Acta Phys. Sin.* **54** 3183 (in Chinese)
- [21] Liu J S and Du Z M 2005 *Acta Phys. Sin.* **54** 2739 (in Chinese)
- [22] Hou C F, Pei Y B, Zhou V X and Sun X D 2005 *Chin. Phys.* **14** 349
- [23] Yeh P 1989 *IEEE J. Quantum Electron.* **25** 484
- [24] Oda I, Otani Y, Liu L and Yoshizawa 1998 *Opt. Commun.* **148** 95
- [25] Vazquez R A, Ewbank M D and Neurgaonkar R R 1991 *Opt. Commun.* **80** 253